ELSEVIER

Sensors and Actuators 77 (1999) 149–156

SENSORS AND ACTUATORS A PHYSICAL

www.elsevier.nl/locate/sna

Micro-stereolithography of polymeric and ceramic microstructures

X. Zhang *, X.N. Jiang, C. Sun

Department of Industrial and Manufacturing Engineering, The Pennsylvania State University, University Park, PA 16802, USA

Received 3 August 1998; accepted 16 March 1999

Abstract

Micro-stereolithography (μSL) is a novel micro-manufacturing process which builds the truly 3D microstructures by solidifying the liquid monomer in a layer by layer fashion. In this work, an advanced μSL apparatus is designed and developed which includes an Ar^+ laser, the beam delivery system, computer-controlled precision x–y–z stages and CAD design tool, and in situ process monitoring systems. The 1.2 μm resolution of μSL fabrication has been achieved with this apparatus. The microtubes with high aspect ratio of 16 and real 3D microchannels and microcones are fabricated on silicon substrate. For the first time, μSL of ceramic microgears has been successfully demonstrated.

Keywords: Stereolithography; MEMS; Micromachining; Microfabrication; Polymer; Ceramics

1. Introduction

As an emerging technology, Micro Electro-Mechanical Systems (MEMS) have drawn worldwide research attention in the last decade. MEMS devices have been found in many sensing applications such as airbag sensors, as well as chemical and biological sensors. In order to develop the intelligent 'micro-system' which is capable of both sensing and actuating, microactuators is the key to making MEMS a fully active device [1]. The microactuators with high output power can be achieved by using real 3D high aspect ratio microstructures [2], adopting novel actuation mechanisms [1,3], and incorporating a broader spectrum of materials into MEMS such as smart ceramics and alloys beyond conventional materials used in IC fabrication [4–6].

Current IC-based micromachining processes used to fabricate MEMS devices have certain limitations in achieving the above goals. First, most of the IC-based micromachining processes cannot be used to fabricate complex 3D micro parts with high aspect ratios. Second, only a few semiconductors and other materials can be processed by the current IC-based micromachining for MEMS. Many other important engineering materials, such as smart ceramics, functional polymer, and metal alloys, cannot be directly incorporated into MEMS through the conventional IC-based micromachining processes. As an alternative, X-ray LIGA (German Lithography, electroforming and molding) process was developed to fabricate microstructures with high aspect ratio [7,8]. However, the X-ray LIGA process has not found a large number of industrial applications due to its limited industrial accessibility and high operational cost. In addition, complex 3D structures cannot be easily achieved by LIGA process. Recently, a new three-dimensional microfabrication technique is developed based on two-photon absorption with micron resolution [9,10]. This approach provides a new way to directly write a 3D microstructure in free form. In the two-photon microfabrication, however, a short-pulsed laser with a high peak-power is required in order to achieve polymerization since the quantum efficiency is quite low. In addition, the two-photon polymerization is limited to the 3D microfabrication from transparent resin, since the laser beam cannot be easily focused inside of the ceramic and metal suspensions. A novel microfabrication process, the μSL was introduced to fabricate high aspect ratio and complex 3D-microstructure [11]. Sophisticated 3D parts can be made by scanning an UV beam on the liquid monomer resin, curing the resin into solid polymer layer by layer, and stacking together all layers with various contours. In contrast to conventional subtractive micromachining, the μSL is an additive process, which enables one to fabricate high aspect ratio microstructures with novel smart materials. The μSL process is, in principle, compatible with silicon processes and batch fabrication is also feasible [12]. The μSL fabrications of micropolymeric parts and subse-

* Corresponding author. Tel.: +1-814-863-3216; Fax: +1-814-863-4745; E-mail: xxz10@psu.edu

0924-4247/99/$ - see front matter
PII: S0924-4247(99)00189-2

quently electro-plating of micrometallic parts have been explored [13–15]. Functional polymer micro parts possess unique characteristics of high flexibility and low density, as well as reasonable electric conductivity in conducting polymers and piezoelectricity in piezo-polymers. Microceramic structures, however, have not been realized yet by μSL, though they are the keys to high temperature and corrosion resistant MEMS devices. Fabrication of 3D complex shape ceramic turbines is critical for microengine application. The finest UV beam spot sizes reported were about 5 μm, which is larger as compared with the resolution of current IC-based micromachining processes. The control of fine line width in μSL is essential to improve the accuracy of micro parts. In this paper, a novel μSL system is designed and developed. The polymer microfabrication on silicon substrate via μSL is investigated to achieve fine line width control. The feasibility of ceramic microfabrications via μSL is explored.

2. μSL

μSL is derived from conventional stereolithography, which is used to fabricate polymer molds in rapid prototyping processes [16]. The basic principle of stereolithography is schematically shown in Fig. 1. A 3D solid model designed with CAD software is sliced into a series of 2D layers with uniform thickness. The NC code generated from each sliced 2D file is then executed to control a motorized x–y stage carrying a vat of UV curable solution. The focused scanning UV beam is absorbed by an UV curable solution consisting of monomer and photoinitiators, leading to the polymerization, i.e., conversion of the liquid monomer to the solid polymer. As a result, a polymer layer is formed according to each sliced 2D file. After one layer is solidified, the elevator moves downward and a new layer of liquid resin can be solidified as the next layer. With the synchronized x–y scanning and the *Z*-axis motion, the complicated 3D micro part is built in a layer by layer fashion. The μSL shares the same principle with its macroscale counterpart, but in different dimensions. In μSL, an UV laser beam is focused to 1–2 μm to solidify a thin layer of 1–10 μm in thickness. Submicron resolution of the x–y–z translation stages and the fine UV beam spot enable precise fabrication of real 3D complex microstructures.

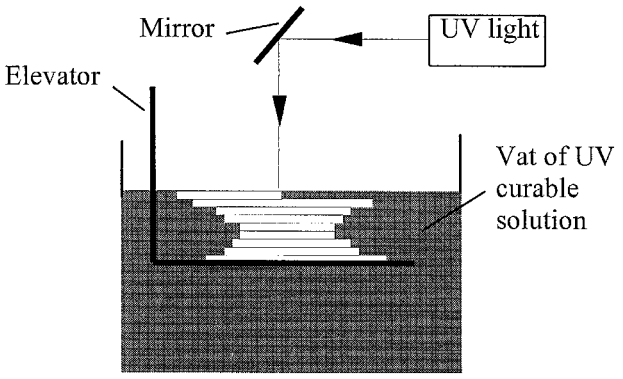

Fig. 1. The principle of stereolithography.

In polymer μSL, the solidified line width and the depth are two important parameters. Upon laser exposure, the photopolymer obeys the Beer–Lambert law of absorption. Earlier macro-scale experiments suggested that the photopolymer has a threshold exposure and curing depth, can be expressed in the following working curve as [16]:

$$C_d = D_p \ln(E/E_c) \quad (1)$$

where C_d is the curing depth, D_p is the penetration depth of the resin defined as $D_p = 1/(2.3\varepsilon[I])$ (ε is the molar extinction coefficient of the initiator, $[I]$ is the initiator concentration), and E and E_c are the laser exposure on the resin surface and critical exposure of the resin at the laser wavelength, respectively. Critical exposure is the laser energy below which the polymerization does not occur. The polymerized line width is described as:

$$L_w = B\sqrt{C_d/(2D_p)} \quad (2)$$

where L_w is the cured line width, and B is the laser spot diameter. The micropolymer structures with different line widths and layer depths can be fabricated by adjusting the laser beam spot size and the exposure energy. For a given UV laser wavelength, the laser exposure is a function of scan speed, laser power and spot size [16].

In Ceramic μSL, an UV curable ceramic suspension is prepared with monomers, photoinitiators and ceramic powders. Upon UV polymerization, the ceramic particles are bonded by the polymer and the ceramic green body is thus formed. The curing depth is found from previous macroscale experiment [17,18] as:

$$C_{cd} \approx \left(\frac{d}{Q}\right)\left(\frac{1}{\Phi}\right)\ln(E/E_c)$$

$$Q = (\Delta n/n_0)^2(d/\lambda)^2 \quad (3)$$

where d is the mean particle size of the ceramic powder, Φ is the volume fraction of ceramics in the suspension, n_0 is the refractive index of the monomer solution, Δn is the refractive index difference between the ceramics and the monomer solution, and λ is the UV wavelength. Compared with the polymer stereolithography, additional factors influence the line width and the curing depth in ceramic stereolithography, such as the particle size and the refractive indexes of the ceramic powder and the solution. Therefore, μSL of microceramic parts is much more complicated than the μSL of pure polymer. It should be noted that the above curing depth and line width relations (Eqs. (1)–(3)) were obtained from macroscopic stereolithography experiments. Their validity in μSL is currently under experimental investigation.

3. Experiments

Experiments were designed to (1) test the constructed μSL apparatus; (2) investigate the μSL of polymeric parts with 3D high aspect ratio; and (3) explore the μSL of ceramic parts for the first time.

An advanced μSL apparatus has been designed and constructed in this work. The μSL apparatus consists of four major parts: an Ar^+ laser, a beam delivery system, computer-controlled precision x–y–z stages and a CAD design tool, and an in situ process monitoring systems. The schematic diagram of the developed μSL apparatus is shown in Fig. 2. The optical setup includes an Ar^+ laser and the beam delivery and focusing optics. As an UV source, the Ar^+ laser was implemented here instead of the UV lamp used in previous work [13,14], in order to obtain a smaller spot size and more stable beam intensity. The scanning control system consists of precision x–y–z stages with 0.5 μm resolution, an elevator attached to the *Z*-axis, and an x–y–z stage controller. A CAD tool provides 3D model design of the microstructures, slicing and the NC code generation. The monitoring system includes a CCD camera, light source and a monitor, which enables one to inspect microfabrication processes in situ. The smallest UV beam spot size achieved was 1–2 μm. The laser wavelength used in this work is 364 nm although two other UV wavelengths, 337 nm and 351 nm, are also available from this Ar^+ laser.

Three UV curable solutions were used in this work: HDDA (the 1,6-hexanediol diacrylate) based resin, aqueous ceramic suspension and non-aqueous ceramic suspension. For polymer microfabrication, the HDDA based UV

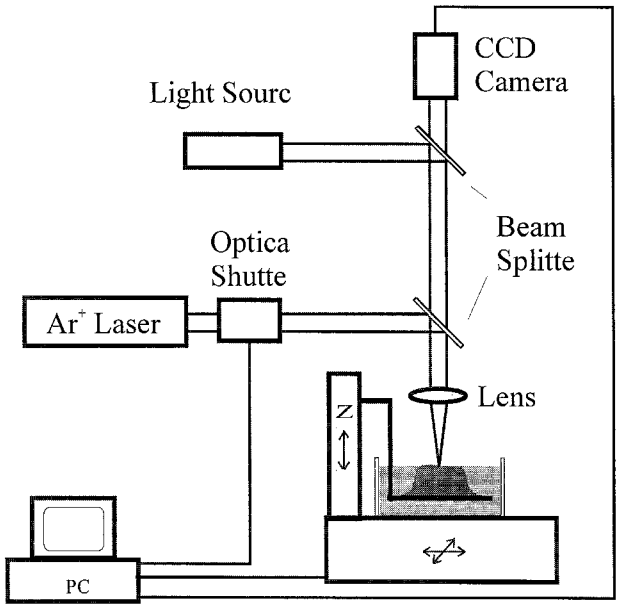

Fig. 2. The μSL apparatus developed at Penn State including an Ar^+ laser, a beam delivery system, computer-controlled precision x–y–z stages and a CAD design tool, and an in situ process monitoring system.

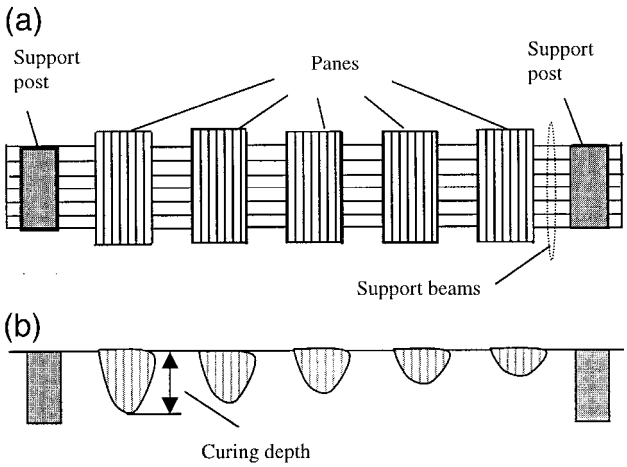

Fig. 3. Micro windowpane structure designed for measurement of the curing depth in μSL of HDDA: (a) top view; (b) side view.

curable resin was prepared, which includes the HDDA monomer and the photoinitiator (benzoin ethyle ether). The photoinitiator was mixed with HDDA for a couple of minutes and fully dispersed after a few hours. The fresh HDDA solution with the photoinitiator concentration of 4 wt.% is transparent, but turns light yellow after exposure to air for more than 24 h. Aqueous ceramic suspension and non-aqueous ceramic suspension were prepared for the ceramic microfabrication [18–20]. The non-aqueous UV curable ceramic suspension contains the HDDA monomer, the photoinitiator, the fine alumina powder (RC-UFX DBM alumina powders), the solvent (DBE, a mixture of dibasic esters) and the dispersant (Triton X-100). The aqueous UV curable ceramic suspension, on the other hand, was prepared with DI water, the monomer (acrylamide and methylenebisacrylamide), the fine alumina powder, the dispersant (Darvan C) and the photoinitiator (Irgacure 2959). The premix solution containing monomer, solvent, photoinitiator and dispersant was prepared first. Subsequently, ceramic powders were added into the premix solution and ball milled for several hours. In this work, the solid loading of the fine alumina powders was about 33% (volume fraction) and the mean particle size of the alumina powders was about 0.2 μm.

The polymerization of the HDDA based resin was characterized under various laser exposures. The micro windowpane experiment was performed for curing depth measurement, as shown in Fig. 3 [16]. Seven parallel support beams work as a bridge between two support posts and five fabricated micropanes are then suspended by the support beams. The support post is 300 μm long, 100 μm wide and 1 mm high. The support beams are 1.76 mm long. Five micropanes designed with the same surface sizes of 400×150 μm were fabricated with different laser exposures, which results in various curing depths. The single line polymerization was also investigated for testing the resolution of the μSL apparatus and the line width

control. In μSL of polymers, both single and multiple layer microstructures were fabricated, including microgears, microchannels, microtubes and microcones with the sizes varying from 100 μm to 1 mm on silicon substrate. The laser power used for μSL of polymer and ceramics was about 5–15 mW. In μSL of ceramics, green bodies of single layer microceramic gears of 400 μm and 1mm were fabricated. The green bodies subsequently went through burn out at temperature of 550–600°C for 2 h. Microceramic gears were finally sintered in the furnace at 1400°C for 3 h in the air environment.

4. Results and discussions

4.1. HDDA polymerization

The micro windowpane structures were fabricated with different laser exposures. The dependence of curing depth on the logarithm of laser exposure is found linear which suggests that microscale polymerization follows the working curve described by Eq. (1) (Fig. 4a). The critical exposure E_c and the penetration depth D_p of HDDA used (the concentration of photoinitiator is 4 wt.%) are determined to be 111 mJ/cm^2 and 242 μm, respectively, through the least square fitting method. For a fixed layer thickness, the polymerized line width increases with laser exposure (Fig. 4b). With a layer thickness of 10 μm, a 1.4 μm thin line was achieved at a laser power of 2.2 μW.

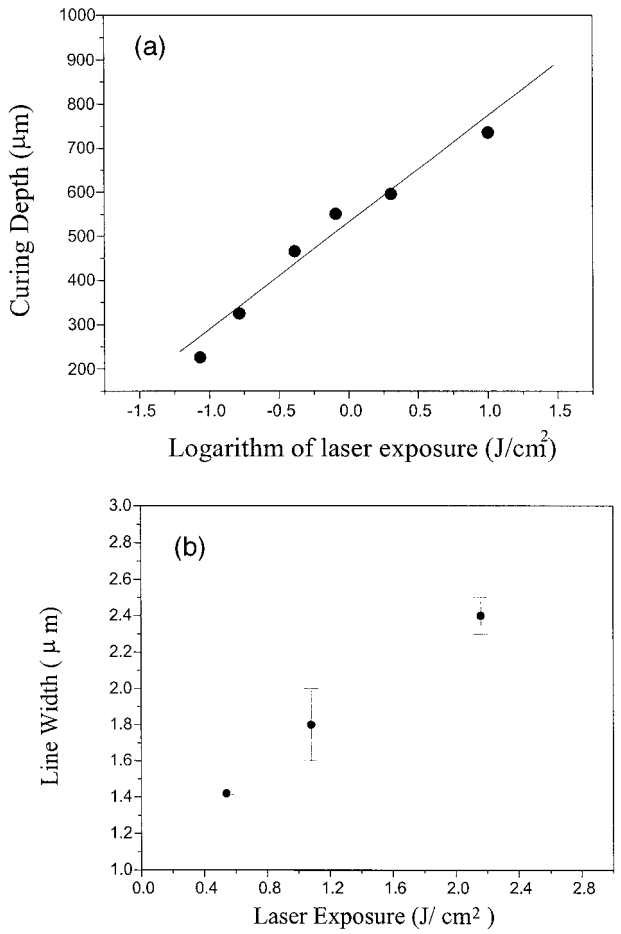

Fig. 4. HDDA UV polymerization characterization: (a) the curing depth dependence on the laser exposure measured from micro windowpane test; (b) the line width dependence on the laser exposure measured from single line scan experiment with confined layer thickness of 10 μm.

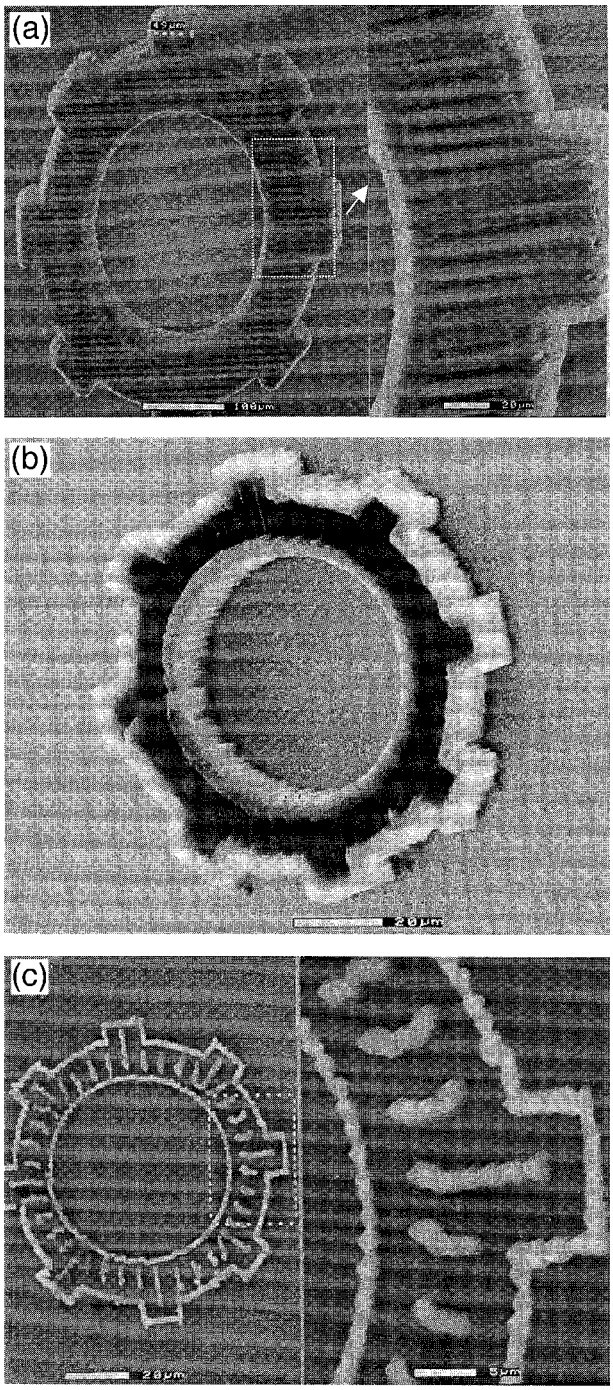

Fig. 5. μSL of single layer polymer (HDDA): (a) 400 μm microgear with the filling line width of 5 μm and the thickness of 30 μm; (b) 100 μm microgear with the thickness of 15 μm; (c) 2 μm line width achieved in 400 μm microgear fabrication.

The finest line obtained in this work is 1.2 μm wide using the developed apparatus.

4.2. μSL of polymers

The single layer polymeric microgears with diameters of 100 and 400 μm were successfully fabricated on silicon substrate by μSL, as shown in Fig. 5. The teeth width is 12.5 μm in 100 μm gears and 50 μm in 400 μm gears. It is observed that the gear shape is well defined with a uniform thickness (Fig. 5a). After fabrication and post-cleaning, an average shrinkage in the microgears is found to be less than 5%. The polymerized line width is found to be about 5 μm as shown in an enlarged section of the fabricated 400 μm gear (Fig. 5a). The space between the two adjacent beam scans is about 8 μm, which is wider than the polymerized 5 μm line, resulting in a 3 μm blank space between the two adjacent solid lines. Good definition is also obtained in the 100 μm microgear fabricated by μSL (Fig. 5b). In both 400 and 100 μm microgears, an overcast layer on the external profiles of the micro parts is observed. The overcast may result from the longer laser exposure on the monomer due to the acceleration and the de-acceleration of the x–y stage at the beginning and the end of each scan pass. As a test of the resolution of the developed apparatus, a microgear with filling lines as fine as 2 μm was fabricated on silicon substrate (Fig. 5c). It is found that controlling the appropriate laser exposure and the beam diameter is the key to achieving high definition in μSL. Factors that influence the laser exposure include the scanning speed, the scanning space between the two adjacent lines, the laser power and the thickness of liquid monomer layer.

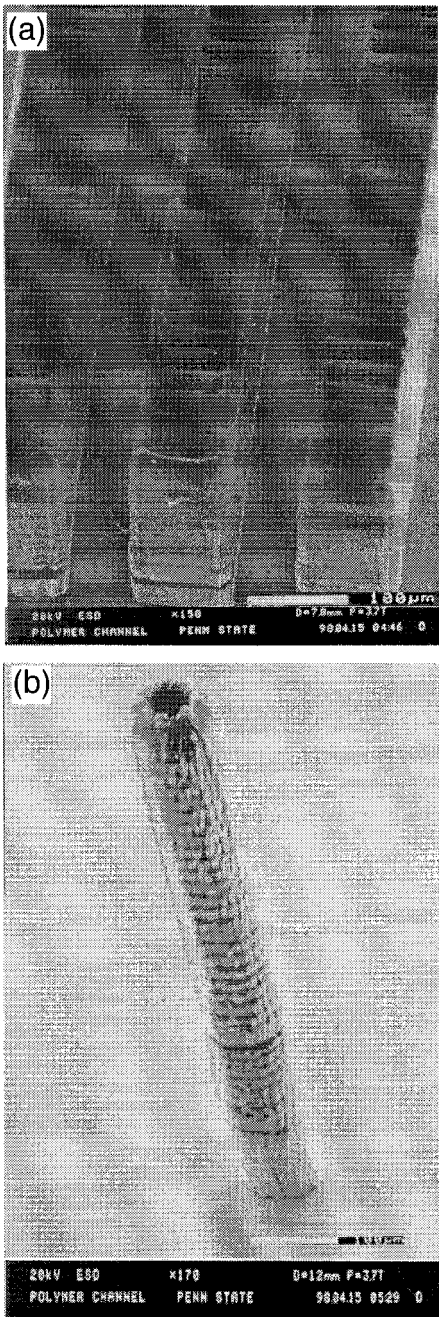

Fig. 6. High aspect ratio micropolymer parts fabricated by multiple layer μSL of HDDA with the layer thickness of 20 μm: (a) microchannels with 100 μm in width and 300 μm in height; (b) a microtube with inner diameter of 50 μm and height of 800 μm.

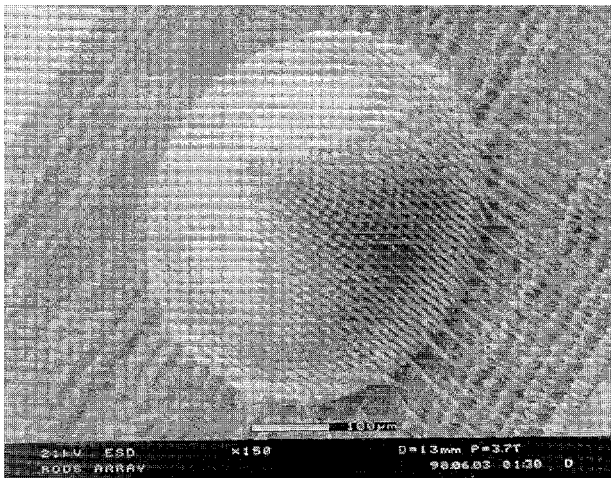

Fig. 7. μSL of 3D complex microstructure: a microcone with bottom diameter of 500 μm and height of 250 μm.

The high aspect ratio microstructures were fabricated with multiple layers by the μSL. Microchannels and a microtube fabricated on silicon substrates are shown in Fig. 6a and b, respectively. The width of the microchannel is 100 μm and the height of the channel is about 300 μm. The microtube has an inner diameter of 50 μm and the total length of 800 μm, which suggests that the aspect ratio of microtube is about 16. Microstructures with even higher aspect ratios can be achieved by μSL due to its layer by layer construction, in contrast to the current IC-based micromachining processes for MEMS. As a 3D microfabrication technique, μSL can form microstructures with complex shapes. A polymer micro convex cone was

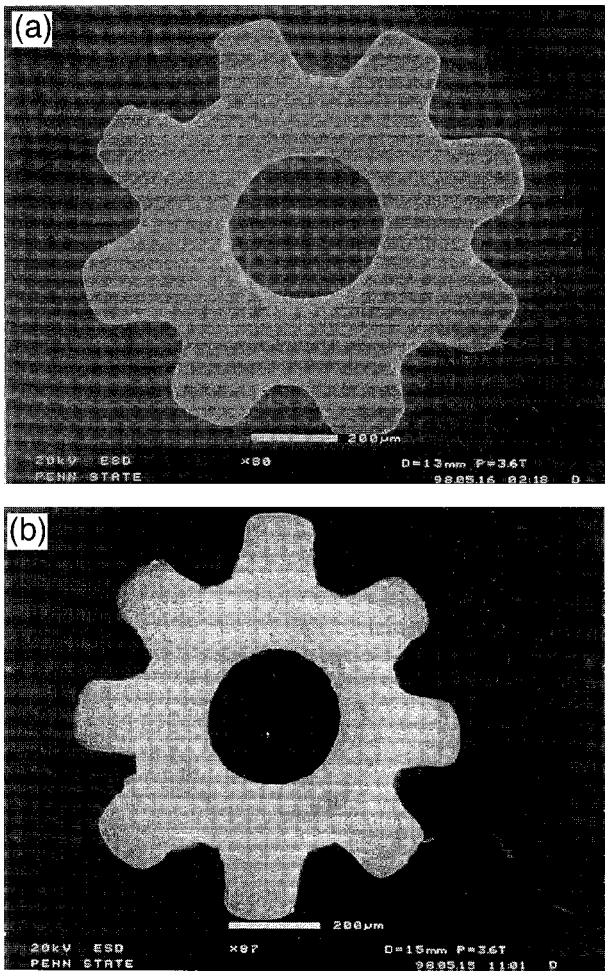

Fig. 8. μSL of ceramics: 1 mm microgear with thickness of 20 μm fabricated from *aqueous* alumina suspension with the solid loading of 33%; (a) Green body after μSL; (b) after 3 h sintering at 1400°C.

fabricated with 25 layers, as shown in Fig. 7, which was constructed. The bottom diameter of the cone is 500 μm and the layer thickness is 10 μm. The demonstrated truly 3D microfabrication capability in the μSL offers great opportunities in design and applications of highly functional microactuators. The single layer fabrication of the microgears (Fig. 5) took less than 1 min. The multiple layer microtube (Fig. 6b) took about 30 min. The rapid fabrication is possible by adjusting the scanning speed and the laser exposure.

4.3. Ceramic microfabrication

For the first time, microceramic structures were successfully fabricated in this work by μSL. The alumina microgears with diameters of 400 and 1000 μm were fabricated from both the aqueous and non-aqueous alumina suspensions with the solid loading of 33% (volume fraction). After fabrication of green body microgears from the aqueous alumina suspension, the burn out and sintering experiments were conducted. The shapes of the alumina microgear before and after sintering are compared in Fig. 8a and b, respectively. The diameter of the alumina microgear decreases from 1032 μm in the green body to 866 μm after sintering. The density of the sintered gear is estimated about 2.2 g/cm^3, which is 56% of the full density (3.9 g/cm^3). This is due to the low solid loading of the suspension and the relatively low sintering temperature (typical sintering temperature of alumina is around 1550–1600°C). Although the linear shrinkage from the sintering is about 16%, the overall shape of the microgear undergoes little change due to the sintering. Higher solid loading in ceramic suspension is expected to result in less shrinkage during sintering. However, the higher solid loading likely leads to higher viscosity of the ceramic suspension which makes the layer thickness control more difficult in μSL [17]. The green bodies of the single layer alumina microgears shown in Fig. 9 were fabricated from the non-aqueous alumina suspension. Compared with their polymer counterparts, the fabricated ceramic gears have a relatively poorer definition. This is mainly due to the UV light scattering by ceramic particles during the laser poly-

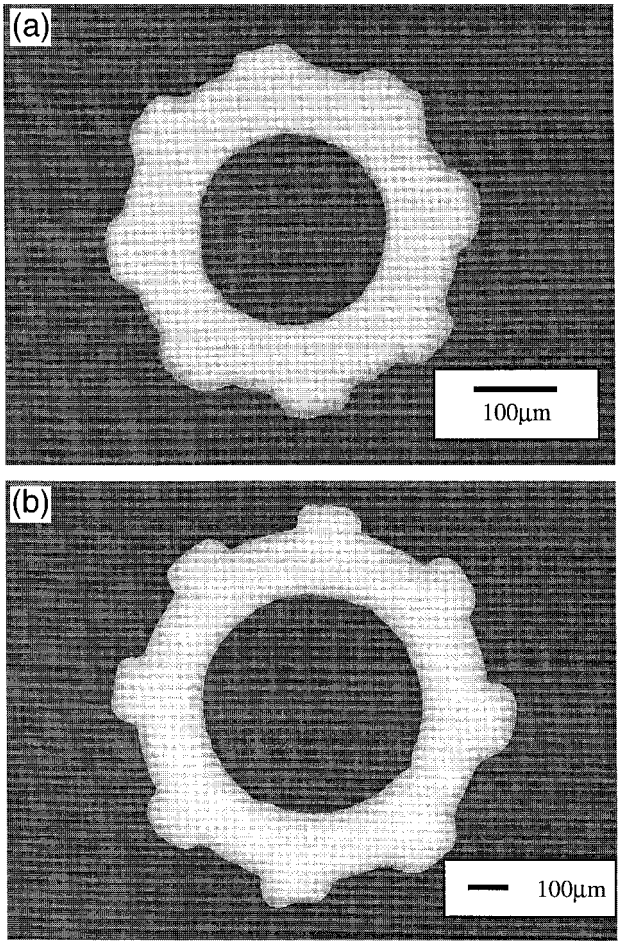

Fig. 9. μSL of ceramic microgears from *non-aqueous* alumina suspension with the solid loading of 33%: (a) 400 μm microgear; (b) 1 mm microgear.

merization of the ceramic suspension. The measured outer diameter of the gear is 1027 μm, which is larger than the designed value of 1000 μm. The thickness of both 1000 and 400 μm single layer gears is about 20 μm. It is also found that a thinner layer of the ceramic suspension results in a better definition since the scattering effect is reduced with decrease of the layer thickness. In order to fabricate the finer ceramic microstructures by μSL, the process optimization of line width and depth is necessary, which includes reduction of the focused beam spot size and the scattering effect from the ceramic suspension [21]. The ceramic suspension with lower viscosity is desirable in μSL because it makes the flow of a thin liquid monomer layer and therefore the layer thickness control easier. At the same solid loading, the viscosity of the aqueous suspension is found to be lower than that of the non-aqueous suspension. However, severe cracks and distortions may occur in the microceramic parts fabricated from aqueous ceramic suspension during post-cleaning and sintering process. The soft cleaning solvent in post-cleaning and the slow temperature ramp-up during the burning and sintering processes are found to be effective to reduce the distortion of microceramic parts fabricated from aqueous suspension. Similar to μSL of ceramic microgears demonstrated in this work, many other important engineering materials such as SMA alloy and metal powders can also be incorporated into μSL. The μSL provides a unique solution to fabricate micro parts with truly 3D complex shapes, high aspect ratios and a wide variety of functional materials.

5. Conclusions

An advanced μSL apparatus was developed, which consists of an Ar^+ laser, a beam delivery system, computer controlled precise x–y–z stages and a CAD design tool, and an in situ process monitoring system. This apparatus is capable of fabricating a line width as fine as 1.2 μm. The successful μSL of microgears, microtubes and micro convex cone structures demonstrated its unique capability of fabrication of micro parts with truly 3D complex shapes, high aspect ratios and a wide variety of functional materials. For the first time, the ceramic microfabrication by μSL was successfully demonstrated. The 400 and 1000 μm microceramic gears were fabricated with reasonable definition. The densified microceramic parts were obtained after the burning and sintering processes.

Acknowledgements

The authors wish to thank Professor Joseph Dougherty and Ms. Mingfang Song of Material Research Laboratory (MRL) at the Pennsylvania State University for the help in ball milling and sintering. The authors also like to acknowledge the following companies for their kind samples supply: alumina powders from Malakoff Industries, TX; solvent from Aldrich Chemical, WI; dispersant from Rohm and Haas, PA and R.T. Vanderbilt, CT; monomer from Sigma, MO; and photoinitiator from Ciba Specialty Chemicals, NY.

References

[1] H. Fujita, Future of actuators and microsystems, Sens. Actuators A 56 (1996) 105–111.
[2] P. Dario, M.C. Carrozza, N. Croce, M.C. Montesi, M. Cocco, Non-traditional technologies for microfabrication, J. Micromech. Microeng. 5 (1995) 64–71.
[3] W.S.N. Trimmer, Microrobots and micromechanical systems, Sens. Actuators 19 (1989) 267–287.
[4] H. Elderstig, O. Larsson, Polymeric MST-high precision at low cost, J. Micromech. Microeng. 7 (1997) 89–92.
[5] G. Kelly, J. Alderman, C. Lyden, J. Barrett, Microsystem packaging: lessons from conventional low-cost IC packaging, J. Micromech. Microeng. 7 (1997) 99–103.
[6] D.L. Polla, L.F. Francis, Ferroelectric thin films in micro-electromechanical systems applications, MRS Bulletin, July 1996, pp. 59–65.
[7] E.W. Becker, W. Ehrfeld, P. Hagmann, A. Maner, D. Muenchmeyer, Fabrication of microstructures with high aspect ratios and great structural heights by synchrotron radiation lithography, Microelectron. Eng. 4 (1) (1986) 35–56.
[8] C. Marques, Y.M. Desta, J. Rogers, M.C. Murphy, K. Kelly, Fabrication of high-aspect-ratio microstructures on planar and nonplanar surfaces using a modified LIGA process, J. Microelectromech. Syst. 6 (4) (1997) 329–336.
[9] S. Maruo, S. Kawata, Two-photon-absorbed near-infrared photopolymerization for three-dimensional microfabrication, J. Microelectromech. Syst. 7 (4) (1998) 411–415.
[10] B.H. Cumpston, J.E. Ehrlich, L.L. Erskine, A.A. Heikal, Z.-Y. Hu, I.-Y.S. Lee, M.D. Levin, S.R. Marder, D.J. McCord, J.W. Perry, H. Rockel, M. Rumi, X.-L. Wu, New photopolymers based on two-photon absorbing chromophores and application to three-dimensional microfabrication and optical storage, Proceedings of the 1997 MRS Fall Meeting, Boston, MA, USA, Dec 1–5, 1997, Vol. 488, pp. 217–225.
[11] K. Ikuta, K. Hirowatari, Real three dimensional microfabrication using stereo lithography and metal molding, Proc. of IEEE MEMS'93 (1993) 42–47.
[12] K. Ikuta, T. Ogata, S. Kojima, Development of mass productive micro stereolithography, Proc. IEEE MEMS'96 (1996) 301–305.
[13] K. Ikuta, K. Hirowatari, T. Ogata, Three dimensional micro integrated fluid systems (MIFS) fabricated by stereo lithography, Proc. IEEE MEMS'94 (1994) 1–6.
[14] S. Maruo, O. Nakamura, S. Kawata, Three-dimensional microfabrication with two-photon-absorbed photopolymerization, Opt. Lett. 22 (2) (1997) 132–134.
[15] S. Maruo, S. Kawata, Two-photon-absorbed photopolymerization for three-dimensional microfabrication, Proc. IEEE MEMS'97 (1997) 169–174.
[16] P.F. Jacobs, Rapid prototyping and manufacturing: fundamentals of stereolithography, Society of Manufacturing Engineers Publishers, Dearborn, 1992.
[17] M.L. Griffith, J.W. Halloran, Stereolithography of ceramics, Proc. of 27th International SAMPE Technical Conference, Albuquerque, NM, USA, Oct 9–12 1995, Vol. 27, pp. 970–979.
[18] M.L. Griffith, J.W. Halloran, Freeform fabrication of ceramics via stereolithography, J. Am. Ceram. Soc. 79 (10) (1996) 2601–2608.

[19] A.C. Young, O.O. Omatete, M.A. Janny, P.A. Menchhofer, Gelcasting of alumina, J. Am. Ceram. Soc. 74 (3) (1991) 612–618.
[20] O.O. Omatete, M.A. Janney, R.A. Strehlow, Gelcasting—a new ceramic forming process, Am. Ceram. Soc. Bull. 70 (10) (1991) 1641–1649.
[21] M.L. Griffith, J.W. Halloran, Scattering of ultraviolet radiation in turbid suspension, J. Appl. Phys. 81 (6) (1997) 2538–2546.

Xiang Zhang graduated with PhD in mechanical engineering from University of California, Berkeley in 1996 and MS/BS in Physics from Nanjing University. He joined Pennsylvania State University in 1996 as an assistant professor and directs Penn State's Micro-manufacturing Laboratory (μML). His past research experiences include: micro thermal wave sensor design and fabrication, ferroelectric liquid crystal phase transition, high-T_c superconductivity, laser processing of semiconductor materials. His current research interests are: 3D micromachining, μSL for MEMS and microsensors and actuators.

Xiaoning Jiang received his PhD from Tsinghua University, Beijing, China in 1996. His PhD thesis is about microfluid flow and the fabrication of micropumps. He joined Nanyang Technological University in Singapore in 1996 as a post-doctoral fellow and worked on microscale cooling for electronics. He is now a post-doctoral scholar at the Micro-manufacturing Laboratory (μML) in the Pennsylvania State University. His current research interests include high aspect ratio microfabrication, microfluidic systems, and smart materials for microactuators and MEMS.

Cheng Sun received his master degree in condensed matter physics in 1996. He is now a PhD student in the industrial and manufacturing engineering department. His major research interest is microfabrication.